Journal of Cell Science 113, 3551-3562 (2000)
Printed in Great Britain © The Company of Biologists Limited 2000
JCS1259

COMMENTARY

Visualizing myosin's power stroke in muscle contraction

Mary C. Reedy

Department of Cell Biology, Duke University Medical Center, Durham, NC 27710, 919 684 5674, USA
(mary.reedy@cellbio.duke.edu)

Published on WWW 4 October 2000

SUMMARY

The long-standing swinging crossbridge or lever arm hypothesis for the motor action of myosin heads finds support in recent results from 3-D tomograms of insect flight muscle (IFM) fast frozen during active contraction and from both fluorescence polarization and X-ray diffraction during rapid stretches or releases of isometrically contracting fibers. The latter provide direct evidence for lever arm movements synchronous with force changes. Rebuilding the atomic model of nucleotide-free subfragment 1 (S1) to fit fast-frozen, active IFM crossbridges suggests a two-stage power stroke in which the catalytic domain rolls on actin from weak to strong binding; this is followed by a 5-nm lever arm swing of the light chain domain, which gives a total interaction distance of approx. 12 nm. Comparison of S1 crystal structures with in situ myosin heads suggests that actin binding may be necessary in order to view the full repertoire of myosin motor action. The differing positions of the catalytic domains of actin-attached myosin heads in contracting IFM suggest that both the actin-myosin binding energy and the hydrolysis of ATP may be used to cock the crossbridge and drive the power stroke.

Movies available on-line:
(http://www.biologists.com/JCS/movies/jcs1259.html)

Key words: Myosin, Muscle, Tomogram, Contraction, Fast freezing, Electron microscopy

INTRODUCTION

Elucidating the structure of myosin motor proteins and the mechanism by which actin-myosin motors transduce the chemical energy of ATP hydrolysis to power the movements of animals and cells remains one of the major challenges in biological science. A host of myosins move intracellular cargo along actin filaments in non-muscle cells, produce the contractions of smooth muscle and drive cytokinesis. Myosin attains its most ambitious functional level acting in the ordered ensembles of muscle, powering such diverse functions as insect flight (at 100 beats/second) or the breaching of a whale.

In this Commentary, I focus on the structure of skeletal muscle myosin II assembled in thick filaments and interacting with actin-containing thin filaments in insect flight and vertebrate striated muscles. Skeletal muscle myosin II consists of two globular heads linked by helical segments that supercoil to form a long helical rod (Fig. 1). The myosin rod segments form the shaft of the thick filaments, and the myosin heads project outward toward the actin thin filaments, forming the myosin crossbridges. Insect flight muscle (IFM) displays myosin heads, in very well-ordered arrangement, bridging between the myosin and actin filaments in 25-nm longitudinal sections that include only a single layer of alternating myosin and actin filaments (the myac layer). I shall place particular emphasis on 3-D tomographic snapshots of myosin freeze-trapped during active contraction in IFM and on how these freeze frames of a power stroke relate to the atomic structures of the myosin head and to the swinging crossbridge or lever arm hypothesis for myosin motor action. Recent reviews that address related topics not discussed here can be found elsewhere (Cooke, 1997; Spudich et al., 1995; Holmes, 1997; Highsmith, 1999; Geeves and Holmes, 1999; Vale and Milligan, 2000; Holmes and Geeves, 2000; Duke, 2000).

A BRIEF HISTORY OF THE SWINGING CROSSBRIDGE OR LEVER ARM HYPOTHESIS

The swinging crossbridge hypothesis for the force-producing mechanism of myosin on actin developed over decades, beginning with the founding observations and insights included in the sliding filament model for muscle contraction co-discovered by H. E. Huxley and A. F. Huxley (Huxley and Hanson, 1954; Huxley and Niedergerke, 1954). In his 1969 review, H. E. Huxley (Huxley, 1969) proposed that the myosin heads projecting from the thick filament interact with actin in the thin filament, and that a change in crossbridge angle or shape coupled to the hydrolysis of MgATP produces sliding between the actin and myosin filaments, which causes muscle force and shortening (Fig. 1).

The demonstration in highly ordered insect flight muscle (IFM) that detached myosin crossbridges are at an approx. 90° angle relative to the long axis of the filaments in ATP-relaxed

IFM and attached at an approx. 45° angle in rigor, the state of high tension and maximal crossbridge attachment in the absence of ATP, supported the idea that the myosin crossbridges act as lever arms during contraction – i.e. that they swing from 90° to 45° following attachment to actin, thereby producing filament sliding and force (Reedy et al., 1965).

Soon after, mechanical experiments on single muscle fibers by A. F. Huxley (Huxley and Simmons, 1971) specified important features of crossbridge behavior. Huxley proposed that crossbridges are independent force generators that interact with actin over a distance of approx. 12 nm in a multi-step power stroke that includes an instantaneous elastic response to a quick release step and an approx. 6 nm or larger active segment in which the myosin 'rolls' over the actin binding site (Huxley, 1974) (Fig. 1). Early models usually treated crossbridges as unitary lever arms whose actin ends served as pivot points as the entire myosin head changed angle. However, Huxley (1974) also suggested that a crossbridge might bend around a internal fulcrum while the part of the crossbridge bound to actin remained stationary **(**Fig. 1).

Huxley and Kress modeled the crossbridge (Huxley and Kress, 1985) as composed of three domains connected by elastic elements, and proposed that it binds to actin over a 12-nm interaction distance and progresses through an evolving actin-myosin interface to end with a short, 4-nm power stroke.

Holmes and collaborators (Holmes et al., 1980; Holmes and Goody, 1984) proposed, on the basis of analysis of X-ray patterns of muscle, that only part of the mass of the myosin head (the 'nose cone') closely follows the actin helix after binding to actin. This would cause only a small intensity increase of the reflections in the X-ray pattern that signal myosin attachment. They further proposed that the nose cone mass remains at a constant angle relative to actin following myosin's initial attachment to actin. This proposal was consistent with the scarcity of a rigor-like, 45° orientation of the mass of the entire myosin head in numerous X-ray diffraction studies of actively contracting muscle. H. E. Huxley commented in a review (Huxley, 1990) that, even though in vitro assays showed that a myosin subfragment 1 (S1) head produces movement (Sheetz and Spudich, 1983; Toyoshima et al., 1987), unambiguous experimental evidence for a change in head configuration or orientation directly linked to force production had not been forthcoming.

Advances in chemical fixation of IFM, combined with X-ray monitoring and 3-D electron tomography (Tregear et al., 1990; Schmitz et al., 1996; Schmitz et al., 1997), produced 3-D images of crossbridges in equilibrium states that were designed to 'drive' bridges backwards through the power stroke from rigor. These approaches used chemical fixation and nucleotide analogs to trap and accumulate myosin heads in conformations that mimic earlier stages of the power stroke. The non-averaging method of 3-D reconstruction provided by tomography was essential for workers to visualize individual variation in myosin head forms, since averaging variable structures 'blurs' the final image. Fig. 2 shows these crossbridge forms with a series of 3-D images. Rigor crossbridges bind in doublet pairs to actin targets every 38.7 nm. The bridges closest or 'leading' toward the M-line (lead bridges) in every 38.7-nm repeat contain both heads of myosin and define the 'classic' 45° axial angle at the end of the power stroke. The bridges closer to the Z-band in the 38.7-nm repeat

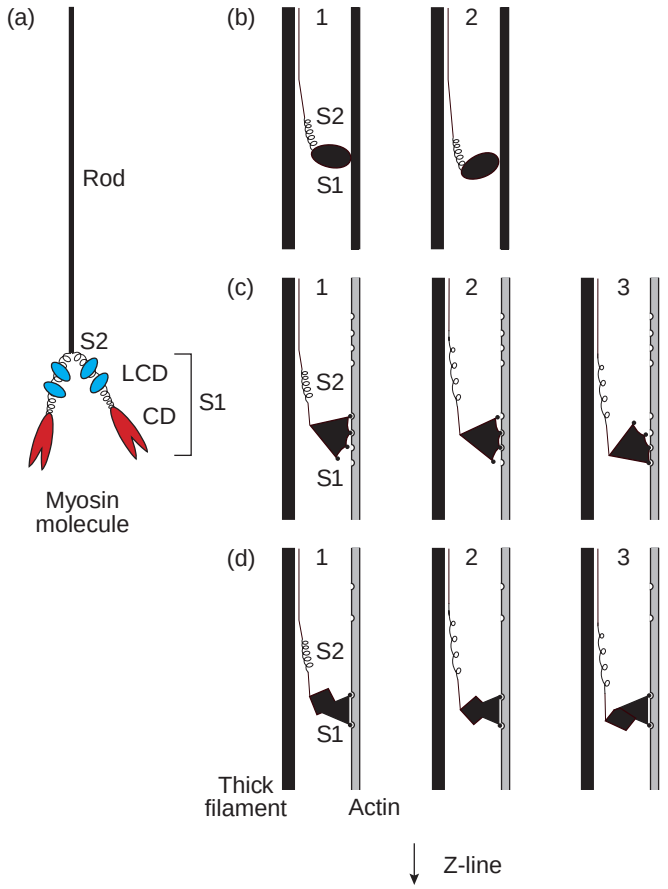

Fig. 1. (a) Schematic diagram of the myosin II molecule. Myosin can be cleaved into several proteolytic subfragments. The myosin head is subfragment 1 (S1) and contains the catalytic domain (CD) and the light chain domain (LCD). The myosin heavy chain folds in the globular CD and extends as an alpha helix through the LCD, to which the essential and regulatory light chains are bound. The two heads connect by a relatively mobile portion of the heavy chain called subfragment 2 (S2) that extends into a long rod segment that is bound into the shaft of the thick filament. (b-d) Schematic diagrams of alternative early models for the postulated crossbridge tilting action during a power stroke. Only one of the two myosin heads is depicted. (b) A myosin head attaches to actin at a 90° angle (1), and the whole head swings to an approx. 45° angle (2) (H. Huxley, 1969). (c) A myosin head attaches to actin at one angle (1) and produces force by rolling over the actin binding site (2) to the end of the power stroke (3). This is a thermal ratchet model (A. Huxley, 1974). The squiggly line represents an elastic element or a spring in the S2. (d) A myosin head attaches to actin at a stable position (1) and bends in the middle (2), producing force and changing the crossbridge angle (3) (A. Huxley, 1974). This is similar to the recent lever arm hypothesis (Rayment et al., 1993b).

(rear bridges) are single-headed and less angled. Ethylene glycol and adenylyl imidodiphosphate (AMPPNP) abolish rigor tension, without reducing rigor stiffness, which indicates that many crossbridges remained attached to actin, probably in a weakly bound state that cannot support tension. 3-D tomograms showed single-headed crossbridges attached to actin at approx. 90° in glycol-AMPPNP, a form that was thought to resemble the initial weak attachment of myosin to actin. Aqueous AMPPNP dramatically reduces tension of IFM,

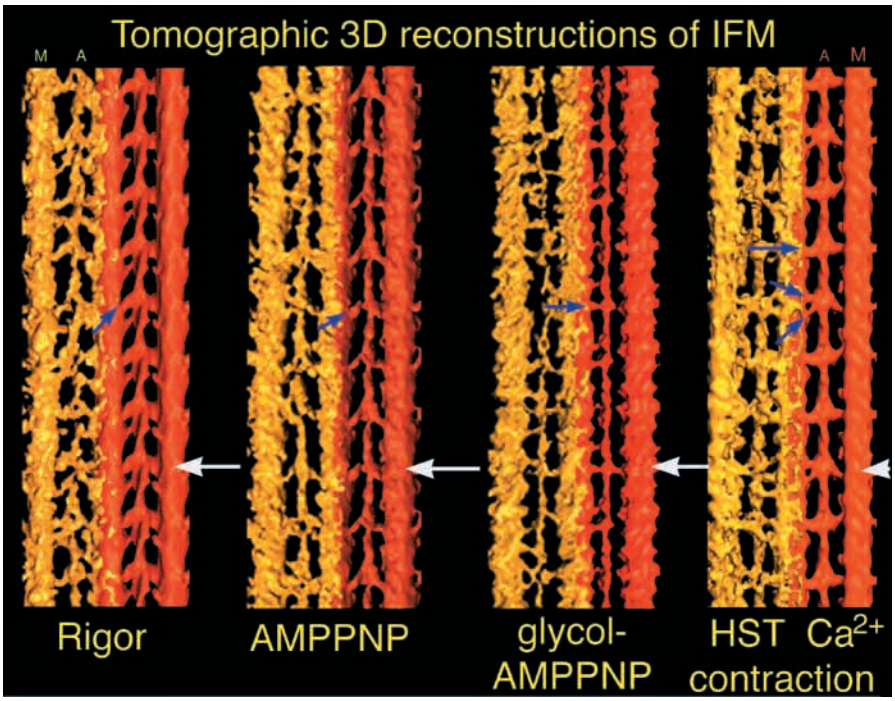

Fig. 2. 3-D tomograms of three equilibrium states of IFM after chemical fixation are compared with freeze-trapped, high static tension (HST), actively contracting IFM. One myac filament repeat, consisting of two myosin thick filaments flanking one actin thin filament, is displayed from each tomogram in longitudinal view. The left side of each panel (yellow) shows a surface rendering of the unaveraged tomogram. The right side (orange) shows the same filament averaged along three crossbridge-actin target axial repeats (3× 38.7 nm = 116 nm), which are aligned in phase with the unaveraged reconstruction. Crossbridge angles show a range (approx. 110°-45°) consistent with a lever arm action of myosin on actin; blue arrows indicate crossbridge angles. In rigor (no ATP), the lead crossbridges (those closest, or leading, to the M-line in each 39-nm repeat) contain both heads of myosin and appear angled at the classic 45° angle at the end of the power stroke. White arrows indicate lead bridge position in the actin target zone in all four panels. The rear bridge (closer to the Z-band in each 39-nm repeat) is single headed and less angled than the lead bridge. In the nucleotide analog AMPPNP, very little axial-angle change was seen in spite of the large drop in tension. However, rear bridges detach and increase 14.5-nm 'shelves' on the thick filament. In ethylene glycol and AMPPNP, the muscle lost all tension but remained very stiff, which indicates crossbridge attachment. Single-headed crossbridges attached in the actin target zone, at a 90° angle that possibly resembled a pre-stroke attachment to actin. Freeze-trapped, freeze-substituted HST contraction showed bridge angles from 110°-45° along a single filament, which suggests bridges are trapped at different stages of an approx. 12-nm power stroke. Single-headed bridges bound in the actin target zone. One bridge form in active contraction suggests a strained crossbridge at the beginning of a power stroke: the V-shaped myosin head. A distinctive crossbridge doublet is seen, which, when complete, is composed of two bridge pairs binding in the same actin target zone in a 39-nm repeat. The bridges closer to the M-line in the doublet reach 'back' to an actin target and are angled at >100°. These are considered to be pre-stroke bridges. The bridges closer to the Z-line are close to the rigor 45° angle at the end of the power stroke and have the same structure as rigor S1. A=Actin filament. M=Myosin filament. M-line is towards the top; Z-band is towards the bottom.

without reducing stiffness. It was expected that the reduction of tension reflected a large step backward in the power stroke, perhaps to 90°. However, actin-attached crossbridges in aqueous AMPPNP remained axially angled near approx. 45°, confounding expectations that they would show a reversal of the power stroke. However, the bridges are less bent and their azimuthal orientation differs from rigor. The crossbridge angles in these chemically fixed, equilibrium states at the beginning and the end of the power stroke are consistent with the idea that crossbridges act as lever arms by tilting to produce force. However, despite these advances, it remained essential to demonstrate different angles of the crossbridge in active, force-producing fibers, and to demonstrate that these angle changes are synchronous with force generation.

PROGRESS FROM X-RAY CRYSTALLOGRAPHY

The solution of the atomic structures of actin (Kabsch et al., 1990) and of myosin S1 (Rayment et al., 1993b) and the building of atomic models for the actin filament (Holmes et al., 1990) and the actomyosin complex (Rayment et al., 1993a) were tremendous achievements and spurred rapid progress on all fronts. Rayment et al. (1993b) revealed the domain structure of the myosin S1 head, showing that the catalytic domain contains the binding sites for actin and ATP at either ends of a long cleft between the upper and lower 50-kDa subdomains, and that the light chain domain (LCD) is composed of a long, heavy-chain helix to which the essential and regulatory light chains bind* (see Fig. 3). They proposed a model for force production in which the overall position of the catalytic domain on actin remains constant as the elongated LCD serves as a lever arm that magnifies small changes accompanying hydrolysis of MgATP (Rayment et al., 1993b). The scissor-like opening and closing of the cleft mechanically links the actin and nucleotide binding sites and controls the movement of the LCD lever arm. This helps open the 'back door' of the nucleotide pocket for release of P_i from ATP hydrolysis (Yount et al., 1995), which signals the onset of the strongly bound part of the power stroke. Closing of the cleft (or 'jaws') on actin is thought to represent strong binding to actin and to affect the position of the LCD lever arm, perhaps locking it in a 'down' position similar to rigor.

Crystallization of a series of *Dictyostelium* myosin catalytic domain constructs (lacking the LCD) with different nucleotides allowed visualization of the changes in conformation around the nucleotide-binding site that occur during ATP hydrolysis.

*In the literature, the catalytic domain is often called the motor domain and the LCD is often termed the regulatory domain or the neck region.

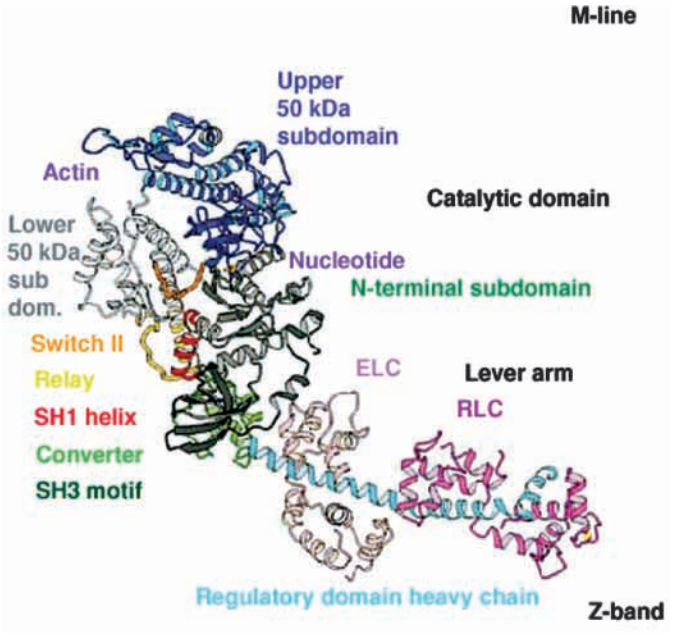

Fig. 3. X-ray crystallographic model of subfragment 1 (S1) from chicken skeletal muscle myosin in the absence of ATP (Rayment et al., 1993). The view is similar to that seen in the tomograms. The atomic model illustrates three key structural elements in the head that change conformation in response to different nucleotides: Switch II (orange); the relay (yellow); and the SH1 helix (red). These three are proposed to control the position of the converter domain (light green) that in turn, controls the different positions of the LCD lever arm, to which the essential (ELC) and regulatory (RLC) light chains are bound. The lower and upper 50-kDa subdomains of the catalytic domain are split by a cleft connecting the actin and nucleotide-binding sites. Modified from Houdusse et al., 1999.

Several showed similar structures to that of S1 without nucleotide or showed similar structures when bound to nucleotides that confer widely different actin-binding affinities in vitro (Fisher et al., 1995a; Fisher et al., 1995b; Smith and Rayment, 1996; Gulick et al., 1997).

Four subdomains have been identified within the myosin catalytic domain: the N-terminal, converter, and upper and lower 50-kDa subdomains (see Fig. 3). The converter (Houdusse and Cohen, 1996) is a mechanical element connecting the catalytic domain to the LCD that amplifies structural changes that accompany nucleotide hydrolysis. Three linking elements have been postulated to be critical to motor function: (1) switch II 'senses' the γ phosphate group of ATP and acts as a gate across the cleft between the upper and lower 50-kDa domains that swings in to partially close the nucleotide binding site and swings out when phosphate is released; (2) the relay helix in the lower 50-kDa subdomain is connected at one end to Switch II and at the other to the converter, and also interacts with the actin-binding site; and (3) the SH1 helix (containing the SH1 and SH 2 sulfhydryls near opposite ends) connects the N-terminal subdomain with the converter and undergoes nucleotide-coupled conformational changes. The converter is connected to the catalytic domain only by the relay and the SH1 helix.

Crystals of smooth muscle myosin constructs that include the catalytic domain and a short portion of the LCD bound to the essential light chain show a position of the 'converter' domain different from that of rigor when MgADP•AlF_4^-(or MgADP•BeF_x) is bound in the nucleotide-binding pocket (Dominguez et al., 1998). The position of the converter domain is tilted approx. 70° relative to that in skeletal S1 without nucleotide, which suggests that if the remainder of the LCD and the regulatory light chain were added, the 'completed' lever arm would be in the pre-power stroke 'up' position relative to the 'down' 45° rigor angle. Holmes modeled a similar pre-stroke configuration based on the *Dictyostelium* catalytic domain structures (Holmes, 1996; Smith and Rayment, 1996). A third position of the converter and LCD was seen in the presence of MgADP in crystals of scallop S1 (Houdusse et al., 1999). In this State III of scallop S1/ADP, the SH1 helix is unwound, the positions of the relay helix and switch II differ from those in State 1 (rigor) and State II (Dominguez pre-stroke), and the converter domain position appears to be unconstrained.

Houdusse et al. (1999) propose that their ADP-bound S1 actually represents the structure of a detached, ATP state of myosin. In the ADP-S1 crystal structure, the unwinding of the SH1 helix brings two cysteine sulfhydryls close (7 Å) together. Other crystal structures show them separated by 18 Å, too far apart to be crosslinked. In states in which these sulfhydryls can be crosslinked, myosin binds only weakly to actin (Bobkova et al., 1999; Nitao and Reisler, 1998). In addition, in Dominguez pre-stroke state II, switch II has moved closer to the 50-kDa cleft at the nucleotide pocket, which is appropriate to a transition state interacting with the γ phosphate group. However, in state III of scallop S1, the cleft is open around the nucleotide, which allows room for ATP in the nucleotide-binding site. The 'jaws' at the actin end of the cleft are also open, which suggests low affinity for actin. Therefore, Houdusse et al. propose that S1 in state III would bind weakly or not at all to actin even though S1-ADP is thought to be a strong binding state* (Houdusse et al., 1999). That the same structure was observed in crystals in the presence of nucleotides that produced different states of myosin in the presence of actin, and in more complete fragments that included the LCD, suggested that interactions within the head or with actin stabilize distinct structures so that they withstand crystal packing forces. Dominguez et al. suggested that MgATP binding could be sufficient to prime the lever arm for a power stroke but that ATP hydrolysis might be necessary to lock the myosin head in the pre-power stroke configuration; they also propose that the essential light chain may stabilize otherwise labile conformations within the catalytic domains (Dominguez et al., 1998). Gulick et al. suggested that myosin head configurations that bind strongly to actin may require actin binding to maintain and display a strong binding configuration in crystals (Gulick et al., 1997). Other evidence also suggests that the actin-binding site, the nucleotide-binding site and the LCD are coupled such that binding of S1 to actin affects the nucleotide site and the LCD and vice versa (Rovner et al., 1995; Sweeney et al., 1998; Kurzawa-Goertz et al., 1998).

*In none of the crystal structures to date are the jaws at the actin end of the 50-kDa cleft closed, even in nucleotide-free S1, which is clearly a strongly bound state in the presence of actin. Rayment et al., nucleotide-free S1 is now referred to as 'near-rigor', because the actin end of the cleft is not closed in the crystal structure. (In unpublished work, Ken Holmes has modelled S1 with the 'jaws' closed on actin.)

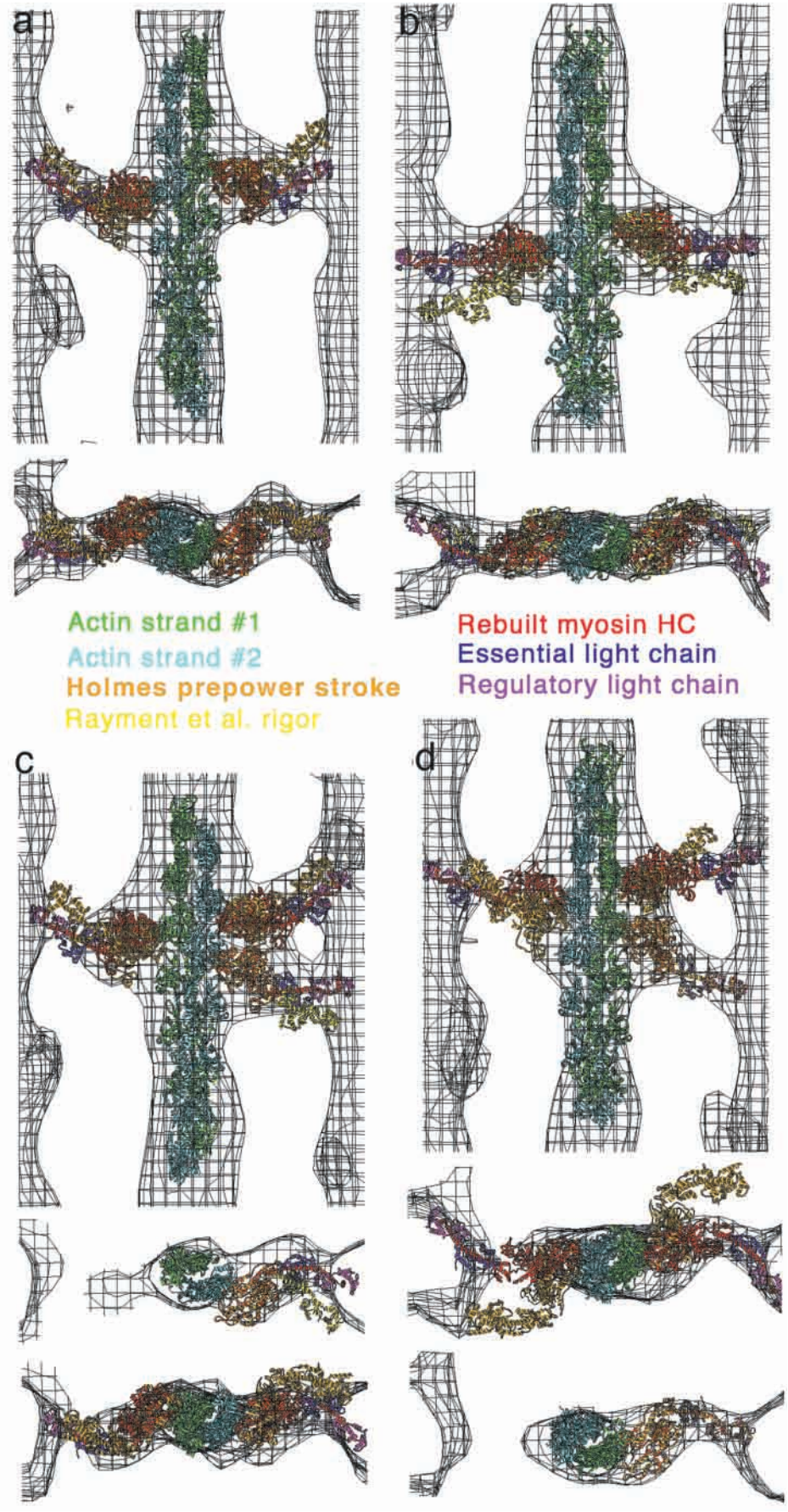

Fig. 4. Acto-S1 atomic model rebuilt to fit averaged crossbridges in the tomogram that represent the full observed range of the power stroke. (a) Pair of approx. 100°, V-shaped crossbridges at the top of the power stroke. The fit of the rebuilt S1 (red) to the crossbridge is compared with the fit of the Holmes pre-stroke model (gold) in longitudinal view (above) and transverse views (below). The LCD of the Holmes pre-stroke model has a slightly higher angle than the crossbridge, but the orientations of catalytic domains of both model and rebuilt S1 are similar and they align well in transverse view. (b) 90° bridge fitted with rebuilt S1 (red) compared to unmodified rigor S1 (yellow) in longitudinal view above, transverse view below. The entire LCD of the bridge is at a 90° angle compared with the 45° angle of rigor S1. The rebuilt S1 and bridge envelope are straighter than rigor S1 in transverse view. (c) Partial doublet with rebuilt S1 (red) compared with rigor S1 (yellow) or pre-stroke model (gold). M-ward and Z-ward denote relative positions of crossbridges with respect to the M-line (towards the top) and the Z-line (towards the bottom). The LCD of the single Z-ward bridge is tilted almost to the rigor angle, whereas the LCDs of both M-ward bridges are angled almost to the pre-stroke angle. Transverse views are below; the Z-ward bridge is uppermost. (d) A partial doublet in which the Z-ward crossbridge is a perfect fit to rigor S1, and the LCDs of the M-ward crossbridges are angled almost up to the pre-stroke model. However, the catalytic domains of the rebuilt S1 of the pre-stroke M-ward bridges do not match the rigor-like position of the Holmes pre-stroke model. Transverse views are shown below; the M-ward crossbridges are uppermost. The entire LCD of the Holmes pre-stroke model lies outside the crossbridge envelope, although the pre-stroke model and the rebuilt S1 are in contact with the same surface on actin. The transverse view of the Z-ward crossbridge matches rigor S1. Color scheme: actin monomers are green and blue; unmodified rigor S1 (Rayment et al., 1993b) is yellow; the rebuild S1 is red; and the unmodified prestroke model (Holmes, 1996) is gold. Longitudinal views are Z-line at the bottom, M-line at the top. Transverse views are shown as if the viewer is looking towards the Z-line.

The LCD can assume a stable and distinct position in response to nucleotide when S1 is bound to actin. Fitting atomic models to 3-D reconstructions of smooth muscle S1 bound to actin in vitro showed a change of LCD position upon release of ADP, past the nucleotide-free rigor position of skeletal myosin (Whittaker et al., 1995). A similar rotation of the LCD lever arm was also detected by use of spin-label probes in smooth muscle (Gollub et al., 1996). Binding to actin seems to connect the clockwork mechanism of relay, switch and converter to stably define the LCD position (Vale and Milligan, 2000). However, ADP addition and removal did not change force in skinned smooth muscle preparations, which led Dantzig et al. to suggest that geometrical constraints of the intact filament lattice alter motions of the myosin heads (Dantzig et al., 1999).

Lever arm motions that are synchronous with force changes in muscle fibers are detected by time-resolved X-ray diffraction and fluorescence polarization.

Elegant results from X-ray diffraction or fluorescent probe studies of muscle fibers provide direct evidence for angle changes of crossbridges that are synchronous with changes in force. Crossbridges move through power strokes asynchronously during isometric contraction. However, very rapid stretches and releases imposed on isometrically contracting fibers can synchronize the working stroke of those crossbridges that are attached to actin. This allows the changes in force and changes in crossbridge angle to be directly related. These achievements depended on improvements in instrumentation, including the development of ultrafast microforce transducers, high-flux X-ray synchrotron beamlines with very efficient detectors and sophisticated new probes and orienting strategies.

Submillisecond time-sliced synchrotron X-ray patterns recorded during rapid stretches and releases of intact vertebrate muscle fibers show changes in intensities that are interpreted as reflecting the tilting of the crossbridges during a power stroke that is synchronous with changes in force due to the length change. The changes in the active force due to crossbridge power strokes follow 1-2 msec after the elastic bending of the bridges that is simultaneous with the length step (Lombardi et al., 1995; Dobbie et al., 1998; Piazzesi et al., 1999).

Bifunctional fluorescent probes attached at two sites are very restricted in mobility; they therefore accurately report the motions of the part of the crossbridge to which they are attached. Fluorescence polarization of multiple probes on the regulatory light chain report axial and azimuthal movements of the LCD that are synchronous with active force changes when rapid length changes are imposed on isometrically contracting muscle fibers (Irving et al., 1995; Allen et al., 1995; Hopkins et al., 1998; Sabido-David et al., 1998; Goldman, 1998; Corrie et al., 1999). Fluorescent probes attached to the catalytic domain on SH1 of the myosin heavy chain reorient when caged nucleotide is released into rigor fibers by photolysis, but changes in catalytic domain position were not observed during rapid length steps (Berger et al., 1996). LCD motion of a single smooth muscle S1 was detected in an in vitro assay by single fluorophore polarization (Warshaw et al., 1998), which suggests that, in the future, polarization signals from a single S1 can be compared with those from large arrays.

Because of uncertainty as to how many myosin heads are reporting these changes in fibers or, in some cases, what direction of motion is being detected, the degree of angle change may be small (approx. 3°) if all heads are reporting or much larger if fewer (approx. 20%) are attached to actin and responding to the length change. Visualization of attached crossbridges in tension-monitored, actively contracting IFM fibers has helped to address this issue.

3-D TOMOGRAPHY OF FAST-FROZEN CONTRACTING IFM

Improved fast freezing/substitution techniques, customized microforce transducers, and 3-D electron tomography that can image variable structures have been combined to capture and visualize working crossbridges in contracting muscle (Taylor et al., 1999). Fast freezing of isometrically contracting IFM represents a unique opportunity to visualize myosin heads producing and bearing tension.

M. K. Reedy and collaborators have linked X-ray diffraction to these techniques to record structural information in the native state, which allows comparison with X-ray diffraction from other muscle types and gives an objective measure of the accuracy of preservation. This gives some assurance that the variety of crossbridge forms and angles seen following freeze substitution in the tomograms reflects native structure. Both tomograms (Taylor et al., 1999) and analysis of intensities of the X-ray diffraction pattern of contracting IFM (Tregear et al., 1998) showed that active crossbridges select helically well-oriented actin targets midway between 38.7-nm-spaced troponins. Both methods indicated that approx. 28% of the myosin heads form single-headed attachments to actin during the high-static-tension state of IFM. Myosin crossbridges in EMs of fast-frozen contracting vertebrate muscle also appear to bind as single heads (Hirose et al., 1994; Hirose and Wakabayashi, 1993). This actin target selectivity and single-headed binding limits the number of heads that bind at one time during isometric contraction. That approx. 28% of the myosin heads attach during isometric contraction in IFM lends support to the view that a small number of crossbridges are attached and reporting in probe and X-ray experiments and, therefore, that the crossbridge angle change is much larger than 3°.

The force measured at the moment of freezing in the IFM fibers processed for tomography represents an average of bridges at different points in the contraction cycle, in contrast to the coordinated lever arm motions mechanically synchronized by rapid stretches and releases. Therefore, the freeze-trapped bridge angles represent positions throughout the power stroke.

The 3-D tomograms of actively contracting IFM fibers showed crossbridge angles from 110° (anti-rigor, or pre-power stroke) through 45° (rigor-like or end of stroke; Fig. 2, fourth panel). If the entire angular range of the LCD swing constitutes the power stroke, it would be approx. 12 nm, the value proposed by Huxley and Simmons (1971). Interestingly, as also observed in vertebrate muscle (Hirose et al., 1994; Lenart et al., 1996), the majority of active crossbridges were at angles closer to 90° than to the rigor 45° angle, which suggests that relatively few bridges are accumulated at the end of their power stroke in a rigor-like conformation. This is also consistent with

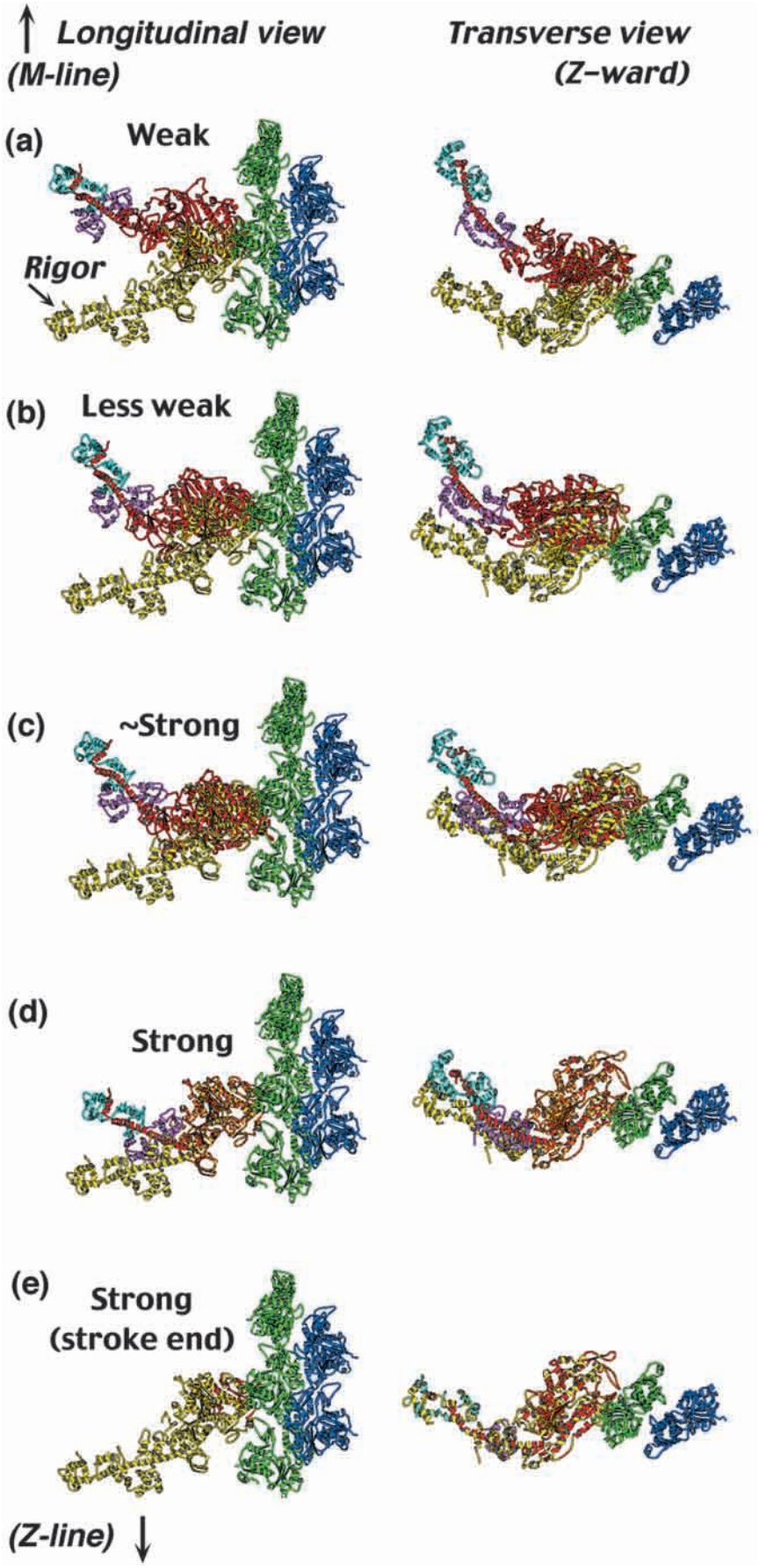

Fig. 5. A hypothetical two-stage power stroke is constructed from a sequence of rebuilt S1s from tomograms of actively contracting IFM. The rebuilt S1s encompass the full range of observed S1 angles and forms and add to a total stroke distance of approx. 12 nm. Each rebuilt S1 is shown in longitudinal view (Z-disk towards the bottom) on the left, and in transverse view on the right (viewed towards the Z-disk). The rebuilt S1 heavy chain is red, the ELC is purple, and the RLC is cyan; the rigor S1 is yellow throughout. Actin is green and blue.
(a) Initial acto-myosin contact, probably weak binding. (b) The catalytic domain (CD) rotates azimuthally and axially on actin, towards the rigor interface. As the CD realigns, the S1 becomes more V shaped. (c) The CD is close to the rigor interface in both axial and azimuthal position, and the LCD is cocked at an anti-rigor angle. Tension may be developing. (d) The CD remains in the rigor orientation on actin, and the LCD begins tilting independently towards 45°. Many S1s and bridges are in this configuration in the tomograms. The angular transition between this and the next LCD position would yield an approx. 5-nm lever arm stroke. (e) The LCD has tilted to the rigor angle and reached the end of the working stroke. This S1 matches rigor S1 perfectly. A movie of these rebuilt S1 motions can be seen at (http://www.biologists.com/JCS/movies/jcs1259.html)

M-line

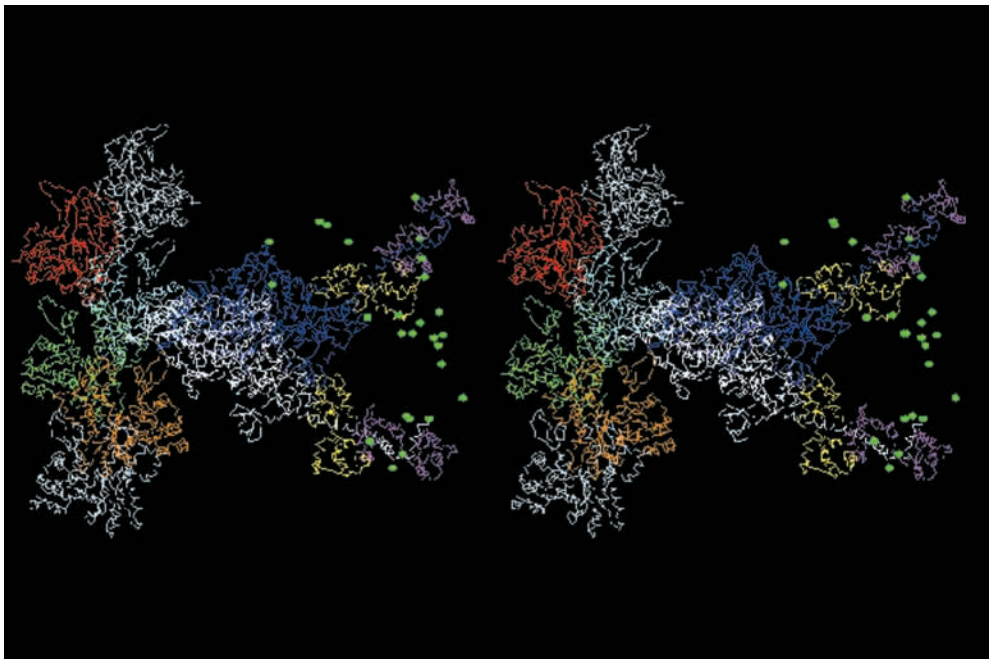

Z-line

Fig. 6. Stereo view in longitudinal orientation of superimposition on one actin monomer of all 26 rebuilt S1s fitted to the high static tension IFM reconstruction. The position of Lys843 at the terminus of the heavy chain is shown as a green dot. For clarity, only one S1 that matched rigor structure is fully shown (representing the end of the power stroke), and only one S1 is shown from the pre-stroke rebuilt S1s. The range of azimuthal orientations of the bridges is broad for the pre-stroke bridges and narrow for those closer to the end of the stroke. The catalytic domain of the prestroke S1 is blue, whereas the rigor catalytic domain is white. The essential light chains are yellow; regulatory light chains are pink. Actin monomer with bound S1 is green, flanked by red or yellow monomers and white actin at each end. The Z-disk would be at the bottom; the M-line would be at the top. Cross-eyed stereo.

X-ray diffraction patterns recorded during active isometric contraction of vertebrate fibers (Piazzesi et al., 1998).

The low-resolution EM images of IFM were related to the atomic structures of isolated myosin heads from X-ray crystallography by rebuilding atomic S1 models to fit freeze-trapped crossbridge density in tomograms. Rebuilding the rigor S1 atomic model (Rayment et al., 1993b) to fit the lower-resolution structures confirmed that the LCD appears to act as a lever arm during force production, as proposed in the Rayment model (Rayment et al., 1993a). The rebuilding of rigor S1 showed that the LCD had to be significantly adjusted to fit the different crossbridges. If only bridges in which the catalytic domain matched the rigor position are considered, this latter part of the range of positions of the LCD would give an approx. 5-nm power stroke. This is consistent with estimates from in vitro assays using S1 myosin heads of an approx. 5-nm step size (Molloy et al., 1995; Block, 1996).

The forms and angles of the crossbridges suggest the following sequence through a two-stage power stroke. In the pre-stroke position (Fig. 4D), the position of the catalytic domain differs azimuthally and axially from that in both rigor S1 and the rigor-like orientation of the catalytic domain of the Holmes pre-stroke model. The LCD of the bridge envelope is highly angled (>100°), which is similar to the Holmes pre-stroke model. Next the catalytic domain rotates down towards the rigor position, but the LCD is still angled ‘up’ (approx. 100°), which confers a ‘V’ shape upon these bridges (Fig. 4A). This bridge form suggests a strained configuration in which it is cocked like a spring at the beginning of a power stroke. The next group of crossbridge forms shows (Fig. 4B and C) the catalytic domain stabilized at the rigor position, and the LCD appears to be at varying angles through a 5 nm lever arm swing. The final group (Fig. 4D) consists of a few bridges that match rigor S1 perfectly. Fig. 5 shows selected S1s that were rebuilt to fit crossbridges arranged in a hypothetical sequence through a two-stage power stroke.

The weakly binding pre-stroke crossbridges show a wide azimuthal variation that narrows as the bridges approach the end of the power stroke. The azimuthal component of movement of the bridges as weak-to-strong binding progresses may help build strain into the heads, tethered as they are in a helical lattice on the thick filament that must link up with actin arrayed in a different helical lattice. AMPPNP, which causes a large drop in tension, did not produce an axial swing of crossbridges in IFM. However, a straightened azimuthal alignment of attached bridges was observed, which suggests that nucleotide binding produces an azimuthal shift of the LCD relative to the catalytic domain that relieves strain**.** Azimuthal variation in the positions of myosin heads is also detected in fluorescence polarization studies and is consistent with the EPR data detecting a disorder-to-order transition of the catalytic domain during the power stroke. Bershitsky et al. (1997) provide evidence from X-ray diffraction and temperature jumps of contracting fibers that azimuthal movement of the catalytic domain is associated with an increase of force, without the change in tilt that accompanies a length step. They interpret the azimuthal shift of catalytic domain position as a weak-to-strong binding transition that allows force to develop. The catalytic domain of crossbridges in the tomograms shows a significant azimuthal shift between the pre-stroke and rigor positions, which is consistent with Bershitsky’s observations. The power stroke sequence in Fig. 5 illustrates a smooth azimuthal transition accompanying the axial angle sequence. However, other fitted S1s deviated from this uniform azimuthal progression. This can be seen in the stereo image in Fig. 6, in which the position of Lys843 of each of the 26 fitted S1s is displayed as a green dot, whereas one pre-stroke and one rigor S1 are fully displayed to mark the beginning and end of the power stroke.

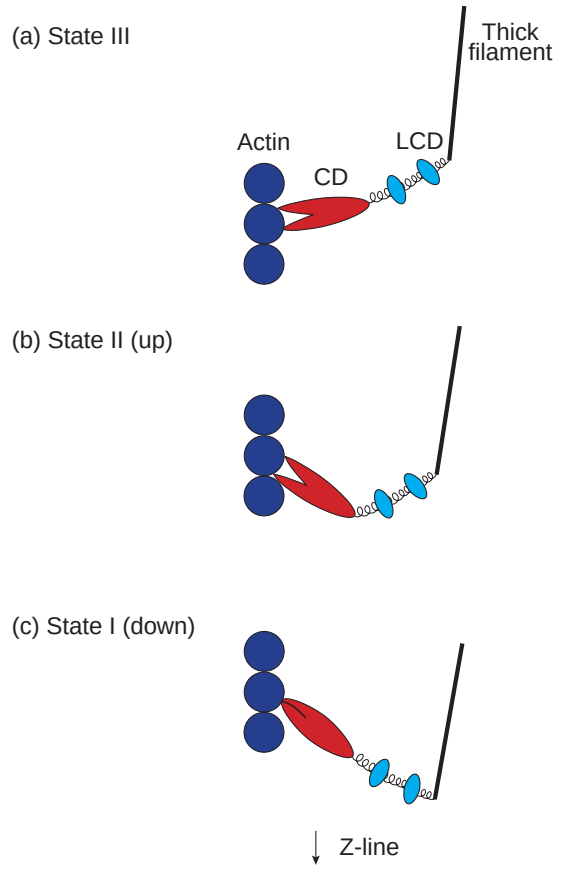

Fig. 7. Schematic diagram showing the possible correspondence between myosin crossbridge forms observed in the actively contracting IFM tomogram and States I, II and III described in X-ray crystallography studies. (a) The most highly angled, weakly bound crossbridges might correspond to State III (Houdusse et al., 1999). This is purely speculative. (b) The V-shaped bridges align well with State II (Holmes, 1997 (based on Smith and Rayment, 1996); Dominguez et al., 1998). The LCD is angled 'up' while the catalytic domain is rotated down to the rigor position. (c) Bridges at the end of the power stroke match rigor S1 well (Rayment et al., 1993a; Rayment et al., 1993b). The LCD is tilted down. Myosin's jaw-like cleft is shown open in (a) and (b) and closed in (c).

A two-stage tilting has been detected in myosin I in in vitro assays (Veigel et al., 1999). The authors suggest this may be due to its slower kinetics relative to skeletal myosin II. A second step was not detected for myosin II, perhaps because it occurs too quickly or because the second step represents a smooth-muscle-like step past the final rigor position of skeletal myosin.

EPR measurements using probes on the catalytic domain and the LCD show independent mobility of these domains of myosin heads during steady-state contraction (Adhikari et al., 1997). EPR of a spin label attached to the regulatory light chain of scallop myosin showed that a large rotation of the LCD occurs during active contraction (Baker et al., 1998). EPR and time-resolved phosphorescence anisotropy (TPA) of probes attached to SH1 in the catalytic domain report that active force generation involves a disorder-to-order transition of the catalytic domain, which suggests that myosin attaches weakly and nonstereospecifically to actin and then undergoes conformational transitions to reach an ordered strong-binding state (Thomas et al., 1995). This is consistent with the transition in position of the catalytic domains seen in freeze-trapped crossbridges.

The 5-nm swing of the LCD lever arm while the catalytic domain is stable at the rigor position, visualized in IFM, and estimated from in vitro assays, is only part of the classic approx. 12-nm power stroke **(**Fig. 7). The transition between the 'up' and 'down' conformations in the crystal structures is proposed to yield an approx. 10-nm force-producing LCD lever arm swing on the assumption that the catalytic domain is in a strong-binding, rigor-like position throughout the stroke. However, fitting of the crystal structures to IFM crossbridges in the tomograms indicates that the catalytic domain position in the highly angled heads is not rigor-like; rather, it suggests weak-binding that may not support force production. Therefore, although the distance over which the crossbridge tilts in IFM is approx. 12 nm, force may not be produced throughout that length.

It remains unclear where State III of scallop S1-ADP might fit in the crossbridge power stroke. It may be an extremely brief intermediate conformation that is difficult to detect. The position of scallop S1 in State III (Houdusse et al., 1999) was illustrated as parallel to the actin filament, largely to keep the actin-binding regions of states I, II and III in the same orientation to actin. Such a position of myosin in muscle has not been seen and appears structurally unlikely given the interfilament spacing, as well as the tethering of each myosin head to its partner and to the thick filament. Clearly, State III S1 would not superimpose on crossbridges near the rigor end of the stroke in the IFM tomograms. However, if the converter domain position is unconstrained in scallop S1-ADP, and it does represent a weakly bound form, it might correspond to some of the weakly bound, pre-stroke crossbridges prior to rotation of the catalytic domain to the strongly bound configuration and consequent bending of the bridge to a V shape (Fig. 7). The prerequisites for a possible alignment with the most 'weakly bound' pre-stroke bridges seem to be that only the upper 50-kDa subdomain portion of the actin-binding site would contact actin, and the LCD would be freely adjusted azimuthally.

The non-rigor angles of the catalytic domain detected in the tomograms contrast with the relatively constant rigor-like orientation of the catalytic domain in the Rayment et al. (1993b) and Holmes (1996) models of the power stroke. In those models, the spring-like cocking of the lever arm into its pre-power stroke conformation is coupled to the binding and hydrolysis of ATP, which occurs while myosin is detached from actin. These steps occur without significant reorientation of the catalytic domain on actin following initial contact. Several X-ray crystal structures for myosin head fragments and S1 are interpreted as consistent with this idea (Smith et al., 1995; Fisher et al., 1995a; Dominguez et al., 1998; Gulick et al., 1997; Houdusse et al., 1999). However, none of these myosin fragments or S1 was bound to actin, tethered to a partner head and to the thick filament, or producing or bearing tension.

Because of coupling between actin binding, nucleotide binding and hydrolysis, and LCD swing, actin binding may be essential if we are to observe the motor action of myosin. The rotation of the catalytic domain after attachment to actin

suggests that myosin heads in situ may not be cocked by ATP hydrolysis for a full power stroke, but require evolution of weak-to-strong actin binding to build strain into the head while the lever arm end is attached to a thick filament. The large actomyosin binding energy may be utilized in skeletal muscle myosin. Cooke (1997) suggested that the formation of the actomyosin bond, which changes from weak to strong binding through broadening of a hydrophobic contact interface by stabilization and suppression of thermal fluctuations, could provide a large portion of the free energy driving the power stroke and that this energy would be distributed in several steps throughout the stroke. This idea is consistent with the changing position of the IFM catalytic domain after attachment.

In thermal-ratchet models (Huxley, 1957) the lever arm gives directionality to the power stroke, which is driven primarily by the binding energy between actin and myosin; ATP binding functions largely to detach myosin from actin. Yanagida et al. (Yanagida et al., 2000a; Yanagida et al., 2000b) propose a biased Brownian ratchet model, on the basis of sophisticated in vitro assays, in which the catalytic domain of myosin binds to two actin monomers at once. The LCD does not act as a lever arm; rather the LCD tilting serves to bias the direction of the processive 'inchworm' movement along the actin helix. The myosin makes several substeps of approx. 5 nm (1-5, depending on the load on the LCD), while hydrolysing only one ATP. The LCD is coupled to the nucleotide- and actin-binding sites such that strain on the LCD affects the kinetics of ATP hydrolysis and actin binding. Elastic energy is stored in the head and is parceled out to fuel the steps. This contrasts with the idea that the hydrolysis of ATP directly produces the energy that drives the force-producing movement of the LCD lever arm, perhaps as suggested by Vale and Milligan (2000) through a clockwork mechanism in which the relay helix serves as a 'piston' that moves the converter and LCD in response to nucleotide-dependent movements of switch II. Uyeda et al. (1996) and Anson et al. (1996) showed that shortening the lever arm slowed the velocity of actin translocation and lengthening the lever arm increased it, as predicted by the lever arm hypothesis. However, Yanagida et al. removed the LCD and reported that although the velocity was slowed, the leverless myosin showed the same displacement (or step) as normal S1 (Yanagida et al., 2000a; Yanagida et al., 2000b).

The structures of in situ myosin heads in the tomograms (Taylor et al., 1999) suggest that active crossbridges in muscle may use both the energy of bond formation to build strain into the head and the energy of ATP hydrolysis to power a clockwork that drives a force-producing lever arm stroke. It is possible that a combination of mechanisms proposed for thermal ratchets and direct force-producing lever arms are operating in myosin heads bound to actin and generating force in muscle.

PERSPECTIVES

Multiple techniques and approaches have produced evidence that the LCD of myosin tilts during force production and supports a view in which the LCD acts as a lever arm to produce force, but many questions remain unanswered. We do not know if the approx. 5-nm value defines the fundamental step length or if myosin generates force over a larger range depending on the circumstances. The discovery of myosin motors that move processively or backwards or are single-headed attests to a multitude of adaptive modifications that confer quite different motor functions. How has the myosin (VI) that moves backwards (Wells et al., 1999) been modified to make the lever arm move in the opposite direction? That myosin V uses both heads to 'walk' processively along actin (De La Cruz et al., 1999; Walker et al., 2000) raises the old question: what does the second head do in skeletal muscle myosin? This is particularly relevant because myosin in contracting muscle appears to use only one head in a crossbridge. Yet myosin with both heads produces greater force and motion than S1 in in vitro assays (Tyska et al., 1999). Force per myosin head is much lower in S1 in in vitro assays (approx. 1.7-4 pN) than the range of force/head calculated for IFM fast frozen fibers (approx. 4-8 pN), depending on how many of the 28% of heads attached are generating tension. An important question about the myosin actin motor is how the internal clockwork revealed by X-ray crystallography is coupled to the cycle of ATP hydrolysis and how these are coupled to lever arm motions when myosin is bound to actin and bearing tension. It is not known whether the closing of the 'jaws' of the 50-kDa cleft on actin is an as-yet-unobserved critical event in a clockwork mechanism driving a direct force-producing tilt of the LCD lever arm. We also do not know whether a rocking or rolling interaction of the catalytic domain with actin and evolution of the acto-myosin interface are equally (or more) important to the power stroke than the demonstrated tilting of the LCD.

Thanks to my collaborators for stimulating discussions and for figures: Ken Taylor for Figs 2, 4 and 5. Michael Reedy for help with Fig. 3, Yale Goldman for Fig. 7. I thank Ken Holmes and the referees for critical reading of the manuscript and helpful comments. Thanks to Lee Sweeney and Anne Houdusse for helpful discussion. This work was supported by NIH grant to Michael Reedy.

REFERENCES

Adhikari, B., Hideg, K. and Fajer, P. G. (1997). Independent mobility of catalytic and regulatory domains of myosin heads. *Proc. Nat. Acad. Sci. USA* **94**, 9643-9647.

Allen, T. S., Sabido-David, C., Ling, N., Irving, M. and Goldman, Y. E. (1995). Transients of fluorescence polarization in skeletal muscle fibers labeled with rhodamine on the regulatory light chain. *Biophys. J.* **68**, 81S-84S.

Baker, J. E., Brust-Mascher, I., Ramachandran, S., LaConte, L. E. and Thomas, D. D. (1998). A large and distinct rotation of the myosin light chain domain occurs upon muscle contraction [see comments]. *Proc. Nat. Acad. Sci. USA* **95**, 2944-2949.

Berger, C. L., Craik, J. S., Trentham, D. R., Corrie, J. E. and Goldman, Y. E. (1996). Fluorescence polarization of skeletal muscle fibers labeled with rhodamine isomers on the myosin heavy chain. *Biophys. J.* **71**, 3330-3343.

Bershitsky, S., Tsaturyan, A., Bershitskaya, O., Mashanov, G., Brown, P., Burns, R. and Ferenczi, M. (1997). Muscle force is generated by myosin heads stereospecifically atttached to actin. *Nature* **388**, 186-190.

Block, S. M. (1996). Fifty ways to love your lever: Myosin motors. *Cell* **87**, 151-157.

Bobkova, E. A., Bobkov, A. A., Levitsky, D. I. and Reisler, E. (1999). Effects of SH1 and SH2 modifications on myosin: similarities and differences. *Biophys. J.* **76**, 1001-1007.

Cooke, R. (1997). Actomyosin interaction in striated muscle. *Physiol. Rev.* **77**, 671-697.

Corrie, J. E., Brandmeier, B. D., Ferguson, R. E., Trentham, D. R., Kendrick-Jones, J., Hopkins, S. C., van der Heide, U. A., Goldman, Y. E., Sabido-David, C., Dale, R. E., Criddle, S. and Irving, M. (1999). Dynamic measurement of myosin light chain domain tilt and twist in musle contraction. *Nature* **400**, 425-430.

Dantzig, J. A., Barsotti, R. J., Manz, S., Sweeney, H. L. and Goldman, Y. E. (1999). The ADP release step of the smooth muscle cross-bridge cycle is not directly associated with force generation. *Biophys. J.* **77**, 386-397.

De La Cruz, E. M., Wells, A. L., Rosenfeld, S. S., Ostap, E. M. and Sweeney, H. L. (1999). The kinetic mechanism of myosin V. *Proc. Nat. Acad. Sci. USA* **96**, 13726-13731.

Dobbie, I., Linari, M., Piazzesi, G., Reconditi, M., Koubassova, N., Ferenczi, M. A., Lombardi, V. and Irving, M. (1998). Elastic bending and active tilting of myosin heads during muscle contraction [see comments]. *Nature* **396**, 383-387.

Dominguez, R., Freyzon, Y., Trybus, K. M. and Cohen, C. (1998). Crystal structure of a vertebrate smooth muscle myosin motor domain and its complex with the essential light chain: visualization of the pre-power stroke state. *Cell* **94**, 559-571.

Duke, T. (2000). Cooperativity of myosin molecules through strain-dependent chemistry. *Phil. Trans. Roy Soc. Lond. B Biol. Sci.* **355**, 529-538.

Fisher, A. J., Smith, C. A., Thoden, J., Smith, R., Sutoh, K., Holden, H. M. and Rayment, I. (1995a). Structural studies of myosin:nucleotide complexes: A revised model for the molecular basis of muscle contraction. *Biophys. J.* **68** (suppl.) 19S-28S.

Fisher, A. J., Smith, C. A., Thoden, J. B., Smith, R., Sutoh, K., Holden, H. M. and Rayment, I. (1995b). X-ray structures of the myosin motor domain of *Dictyostelium discoideum* complexed with MgADP•BeF_x and MgADP•AlF_4^-. *Biochemistry* **34**, 8960-8972.

Geeves, M. A. and Holmes, K. C. (1999). Structural mechanism of muscle contraction. *Annu. Rev. Biochem.* **68**, 687-728.

Goldman, Y. E. (1998). Wag the tail: structural dynamics of actomyosin. *Cell* **93**, 1-4.

Gollub, J., Cremo, C. R. and Cooke, R. (1996). ADP release produces a rotation of the neck region of smooth myosin but not skeletal myosin. *Nature Struct. Biol.* **3**, 796-802.

Gulick, A. M., Bauer, C. B., Thoden, J. B. and Rayment, I. (1997). X-ray structures of the MgADP, MgATPgammaS and MgAMPPNP complexes of the Dictyostelium discoideum myosin motor domain. *Biochemistry* **36**, 11619-11628.

Highsmith, S. (1999). Lever arm model of force generation by actin-myosin-ATP. *Biochemistry* **38**, 9791-9797.

Hirose, K. and Wakabayashi, T. (1993). Structural change of crossbridges of rabbit skeletal muscle during isometric contraction. *J. Muscle Res. Cell Motil.* **14**, 432-445.

Hirose, K., Franzini-Armstrong, C., Goldman, Y. E. and Murray, J. M. (1994). Structural changes in muscle crossbridges accompanying force generation. *J. Cell Biol.* **127**, 763-778.

Holmes, K. C., Tregear, R. T. and Barrington Leigh, J. (1980). Interpretation of the low angle X-ray diffraction from insect muscle in rigor. *Proc. Royal Soc. Lond. B Biol.* **207**, 13-33.

Holmes, K. C. and Goody, R. S. (1984). The nature of the actin cross-bridge interaction. *Advan. Exp. Med. Biol.* **170**, 373-384.

Holmes, K. C., Popp, D., Gebhard, W. and Kabsch, W. (1990). Atomic model of the actin filament. *Nature* **347**, 44-49.

Holmes, K. C. (1996). Muscle proteins–their actions and interactions. *Curr. Opin. Struct. Biol.* **6**, 781-789.

Holmes, K. C. (1997). The swinging lever-arm hypothesis of muscle contraction. *Curr. Biol.* **7**, R112-118.

Holmes, K. C. ad Geeves, M. A. (2000). The structural basis of muscle contraction. *Phil. Trans. Roy Soc. Lond. B Biol.* **355**, 419-431.

Hopkins, S. C., Sabido-David, C., Corrie, J. E., Irving, M. and Goldman, Y. E. (1998). Fluorescence polarization transients from rhodamine isomers on the myosin regulatory light chain in skeletal muscle fibers. *Biophys. J.* **74**, 3093-3110.

Houdusse, A. and Cohen, C. (1996). Structure of the regulatory domain of scallop myosin at 2 Å resolution: Implications for regulation. *Structure* **4**, 21-32.

Houdusse, A., Kalabokis, V. N., Himmel, D., Szent-Gyorgyi, A. G. and Cohen, C. (1999). Atomic structure of scallop myosin subfragment S1 complexed with MgADP: a novel conformation of the myosin head [In Process Citation]. *Cell* **97**, 459-470.

Huxley, A. F. and Niedergerke, R. (1954). Structural changes in muscle during contraction. *Nature* **173**, 971-973.

Huxley, A. F. (1957). Muscle structure and theories of contraction. *Prog. Biophys. Biophys. Chem.* **7**, 255-318.

Huxley, A. F. and Simmons, R. M. (1971). Proposed mechanism of force generation in striated muscle. *Nature* **233**, 533-538.

Huxley, A. F. (1974). Muscular contraction. *J. Physiol.* **243**, 1-43.

Huxley, H. E. and Hanson, J. (1954). Changes in the cross-striations of muscle during contraction and stretch and their structural interpretation. *Nature* **173**, 973-976.

Huxley, H. E. (1969). The mechanism of muscular contraction. *Science* **164**, 1356-1366.

Huxley, H. E. and Kress, M. (1985). Crossbridge behaviour during muscle contraction. *J. Muscle Res. Cell Motil.* **6**, 153-161.

Huxley, H. E. (1990). Sliding filaments and molecular motile systems. *J. Biol. Chem.* **265**, 8347-8350.

Irving, M., St Claire Allen, T., Sabido-David, C., Craik, J. S., Brandmeier, B., Kendrick-Jones, J., Corrie, J. E. T., Trentham, D. R. and Goldman, Y. E. (1995). Tilting of the light-chain region of myosin during step length changes and active force generation in skeletal muscle. *Nature* **375**, 688-691.

Kabsch, W., Mannherz, H. G., Suck, D., Pai, E. F. and Holmes, K. C. (1990). Atomic structure of the actin: DNase I complex. *Nature* **347**, 37-44.

Kurzawa-Goertz, S. E., Perreault-Micale, C. L., Trybus, K. M., Szent-Gyorgyi, A. G. and Geeves, M. A. (1998). Loop I can modulate ADP affinity, ATPase activity and motility of different scallop myosins. Transient kinetic analysis of S1 isoforms. *Biochemistry* **37**, 7517-7525.

Lenart, T. D., Murray, J. M., Franzini-Armstrong, C. and Goldman, Y. E. (1996). Structure and periodicities of crossbridges in relaxation and during contraction initiated by photolysis of caged calcium. *Biophys. J.* **71**, 2289-2306.

Lombardi, V., Piazzesi, G., Ferenczi, M. A., Thirlwell, H., Dobbie, I. and Irving, M. (1995). Elastic distortion of myosin heads and repriming of the working stroke in muscle. *Nature* **374**, 553-555.

Molloy, J. E., Burns, J. E., Kendrick-Jones, J., Tregear, R. T. and White, D. C. (1995). Movement and force produced by a single myosin head [see comments]. *Nature* **378**, 209-212.

Nitao, L. K. and Reisler, E. (1998). Probing the conformational states of the SH1-SH2 helix in myosin: a cross-linking approach. *Biochemistry* **37**, 16704-16710.

Piazzesi, G., Koubassova, N., Irving, M. and Lombardi, V. (1998). On the working stroke elicited by steps in length and temperature. *Advan. Exp. Med. Biol.* **453**, 259-263.

Piazzesi, G., Reconditi, M., Dobbie, I., Linari, M., Boesecke, P., Diat, O., Irving, M. and Lombardi, V. (1999). Changes in conformation of myosin heads during the development of isometric contraction and rapid shortening in single frog muscle fibres. *J. Physiol. (Lond).* **514**, 305-312.

Rayment, I., Holden, H. M., Whittaker, M., Yohn, C. B., Lorenz, M., Holmes, K. C. and Milligan, R. A. (1993a). Structure of the actin-myosin complex and its implications for muscle contraction. *Science* **261**, 58-65.

Rayment, I., Rypniewsky, W. R., Schmidt-Bäse, K., Smith, R., Tomchick, D. R., Benning, M. M., Winkelmann, D. A., Wesenberg, G. and Holden, H. M. (1993b). Three-dimensional structure of myosin subfragment-1: a molecular motor. *Science* **261**, 50-58.

Reedy, M. K., Holmes, K. C. and Tregear, R. T. (1965). Induced changes in orientation of the cross-bridges of glycerinated insect flight muscle. *Nature* **207**, 1276-1280.

Rovner, A. S., Freyzon, Y. and Trybus, K. M. (1995). Chimeric substitutions of the actin-binding loop activate dephosphorylated but not phosphorylated smooth muscle heavy meromyosin. *J. Biol. Chem.* **270**, 30260-30263.

Sabido-David, C., Brandmeier, B., Craik, J. S., Corrie, J. E., Trentham, D. R. and Irving, M. (1998). Steady-state fluorescence polarization studies of the orientation of myosin regulatory light chains in single skeletal muscle fibers using pure isomers of iodoacetamidotetramethylrhodamine. *Biophys. J.* **74**, 3083-3092.

Schmitz, H., Reedy, M. C., Reedy, M. K., Tregear, R. T., Winkler, H. and Taylor, K. A. (1996). Electron tomography of insect flight muscle in rigor and AMPPNP at 23°C. *J. Mol. Biol.* **264**, 279-301.

Schmitz, H., Reedy, M. C., Reedy, M. K., Tregear, R. T. and Taylor, K. A. (1997). Tomographic three-dimensional reconstruction of insect flight muscle partially relaxed by AMPPNP and ethylene glycol. *J. Cell Biol.* **139**, 695-707.

Sheetz, M. P. and Spudich, J. A. (1983). Movement of myosin-coated fluorescent beads on actin cables in vitro. *Nature* **303**, 31-35.

Smith, C. A., Fisher, A. J., Smith, R., Sutoh, K. and Rayment, I. (1995).

The structure of the ATP-bound state of myosin. *J. Muscle Res. Cell Motil.* **16**, 145.

Smith, C. A. and Rayment, I. (1996). X-ray structure of the magnesium(II). ADP. vanadate complex of the *Dictyostelium discoideum* myosin motor domain to 1. 9 Å resolution. *Biochemistry* **35**, 5404-5417.

Spudich, J. A., Finer, J., Simmons, B., Ruppel, K., Patterson, B. and Uyeda, T. (1995). Myosin structure and function. *Cold Spring Harbor Symp. Quant. Biol.* **60**, 783-791.

Sweeney, H. L., Rosenfeld, S. S., Brown, F., Faust, L., Smith, J., Xing, J., Stein, L. A. and Sellers, J. R. (1998). Kinetic tuning of myosin via a flexible loop adjacent to the nucleotide binding pocket. *J. Biol. Chem.* **273**, 6262-6270.

Taylor, K. A., Schmitz, H., Reedy, M. C., Goldman, Y. E., Franzini-Armstrong, C., Sasaki, H., Tregear, R. T., Poole, K. J. V., Lucaveche, C., Edwards, R. J., Chen, L. F., Winkler, H. and Reedy, M. K. (1999). Tomographic 3-D reconstruction of quick frozen, Ca^{2+}-activated contracting insect flight muscle. *Cell* **99**, 421-431.

Thomas, D. D., Ramachandran, S., Roopnarine, O., Hayden, D. W. and Ostap, E. M. (1995). The mechanism of force generation in myosin: A disorder-to-order transition, coupled to internal structural changes. *Biophys. J.* **68** (suppl.) 135S-141S.

Toyoshima, Y. Y., Kron, S. J., McNally, E. M., Niebling, K. R., Toyoshima, C. and Spudich, J. A. (1987). Myosin subfragment-1 is sufficient to move actin filaments in vitro. *Nature* **328**, 536-539.

Tregear, R. T., Wakabayashi, K., Tanaka, H., Iwamoto, H., Reedy, M. C., Reedy, M. K., Sugi, H. and Amemiya, Y. (1990). X-ray diffraction and electron microscopy from *Lethocerus* flight muscle partially relaxed by adenylylimidodiphosphate and ethylene glycol. *J. Mol. Biol.* **214**, 129-141.

Tregear, R. T., Edwards, R. J., Irving, T. C., Poole, K. J. V., Reedy, M. C., Schmitz, H., Towns-Andrews, E. and Reedy, M. K. (1998). X-ray diffraction indicates that active crossbridges bind to actin target zones in insect flight muscle. *Biophys. J.* **74**, 1439-1451.

Tyska, M. J., Dupuis, D. E., Guilford, W. H., Patlak, J. B., Waller, G. S., Trybus, K. M., Warshaw, D. M. and Lowey, S. (1999). Two heads of myosin are better than one for generating force and motion. *Proc. Nat. Acad. Sci. USA* **96**, 4402-4407.

Uyeda, T., Abramson, P. and Spudich, J. (1996). The neck region of the myosin motor domain acts as a lever arm to generate movement. *Proc. Nat. Acad. Sci. USA* **93**, 4459-4464.

Vale, R. D. and Milligan, R. A. (2000). The way things move: looking under the hood of molecular motor proteins. *Science* **288**, 88-95.

Veigel, C., Coluccio, L. M., Jontes, J. D., Sparrow, J. C., Milligan, R. A. and Molloy, J. E. (1999). The motor protein myosin-I produces its working stroke in two steps [see comments]. *Nature* **398**, 530-533.

Walker, M., Burgess, S., Sellers, J., Wang, F., Hammer, J., Trinick, J. and Knight, P. (2000). Two-headed binding of a processive myosin to F-actin. *Nature* **405**, 804-807.

Warshaw, D. M., Hayes, E., Gaffney, D., Lauzon, A. M., Wu, J., Kennedy, G., Trybus, K., Lowey, S. and Berger, C. (1998). Myosin conformational states determined by single fluorophore polarization. *Proc. Nat. Acad. Sci. USA* **95**, 8034-8039.

Wells, A. L., Lin, A. W., Chen, L. Q., Safer, D., Cain, S. M., Hasson, T., Carragher, B. O., Milligan, R. A. and Sweeney, H. L. (1999). Myosin VI is an actin-based motor that moves backwards [see comments]. *Nature* **401**, 505-508.

Whittaker, M., Wilson-Kubalek, E. M., Smith, J. E., Faust, L., Milligan, R. A. and Sweeney, H. L. (1995). A 35-Å movement of smooth muscle myosin on ADP release. *Nature* **378**, 748-751.

Yanagida, T., Kitamura, K., Tanaka, H., Iwane, A. H. and Esaki, S. (2000a). Single molecule analysis of the actomyosin motor. *Curr. Opin. Cell Biol.* **12**, 20-25.

Yanagida, T., Esaki, S., Iwane, A. H., Inoue, Y., Ishijima, A., Kitamura, K., Tanaka., H. and Tokunaga, M. (2000b). Single-motor mechanics and models of the myosin motor. *Phil. Trans Roy. Soc. Lond. B Biol.* **355**, 441-447.

Yount, R. G., Lawson, D. and Rayment, I. (1995). Is myosin a 'back door' enzyme? *Biophys. J.* **68** (suppl.) 44S-49S.